HHS Public Access

Author manuscript

Cell Rep. Author manuscript; available in PMC 2016 April 07.

Published in final edited form as:

Cell Rep. 2015 April 7; 11(1): 125–136. doi:10.1016/j.celrep.2015.03.010.

mTORC2 regulates cardiac response to stress by inhibiting MST1

Sebastiano Sciarretta[1,2], **Peiyong Zhai**[1], **Yasuhiro Maejima**[1], **Dominic P. Del Re**[1], **Narayani Nagarajan**[1], **Derek Yee**[1], **Tong Liu**[3], **Mark A. Magnuson**[4,5], **Massimo Volpe**[2,6], **Giacomo Frati**[2,7], **Hong Li**[3], and **Junichi Sadoshima**[1,8]

[1]Cardiovascular Research Institute, Department of Cell Biology and Molecular Medicine, Rutgers–New Jersey Medical School, Newark, New Jersey, USA, 07103

[2]IRCCS Neuromed, Pozzilli (IS), Italy, 86077

[3]Center for Advanced Proteomics Research, Rutgers–New Jersey Medical School, Newark, New Jersey, USA

[4]Center for Stem Cell Biology, Vanderbilt University School of Medicine, Nashville, TN 37232, USA

[5]Department of Molecular Physiology and Biophysics, Vanderbilt University School of Medicine, Nashville, TN 37232, USA

[6]Division of Cardiology, Department of Clinical and Molecular Medicine, Faculty of Medicine and Psychology, University "Sapienza", Rome, Italy, 00187

[7]Department of Medico-Surgical Sciences and Biotechnologies, University “Sapienza”, Latina, Italy, 04100

Summary

The mTOR and Hippo pathways have recently emerged as the major signaling transduction cascades regulating organ size and cellular homeostasis. However, direct crosstalk between two pathways is yet to be determined. Here we demonstrate that mTORC2 is a direct negative regulator of the MST1 kinase, a key component of the Hippo pathway. mTORC2 phosphorylates

[8]Address correspondence to: Junichi Sadoshima, MD, PhD, Cardiovascular Research Institute, Rutgers–New Jersey Medical School, 185 South Orange Avenue, Medical Science Building, G-609, Newark, New Jersey 07103, USA. Phone: (973) 972-8619; Fax: (973) 972-8919; sadoshju@njms.rutgers.edu.

Author contributions

S.S. designed and performed experiments, analyzed data and wrote the manuscript; P.Z. performed animal surgery; T.L. and H.L. performed experiments and analyzed data regarding proteomic analyses; Y.M, D.P.D.R., N.N. and D.Y. performed experiments, analyzed data and critically revised the manuscript; M.M. provided the animals and critically revised the manuscript; M.V. and G.F. supervised the project and critically revised the manuscript; J.S. supervised the project, designed the studies, analyzed the data and wrote the manuscript.

Disclosures

None.

MST1 at serine 438 in the SARAH domain, thereby reducing its homodimerization and activity. We found that Rictor/mTORC2 preserves cardiac structure and function by restraining the activity of MST1 kinase. Cardiac-specific mTORC2 disruption through rictor deletion leads to a marked activation of MST1 that, in turn, promotes cardiac dysfunction and dilation, impairing cardiac growth and adaptation in response to pressure overload. In conclusion, our study demonstrates the existence of a direct crosstalk between mTORC2 and MST1 that is critical for cardiac cell survival and growth.

Keywords

Rictor; mTORC2; MST1; Hippo signaling; heart

Introduction

Cellular growth, proliferation and survival are critical processes that must be finely regulated in order to preserve the structure and function of different organs. The Mechanistic (previously called mammalian) Target of Rapamycin (mTOR) and Hippo pathways have recently emerged as the major signaling transduction cascades regulating organ size and cellular survival. The mTOR pathway promotes protein synthesis, cellular growth and survival (Laplante and Sabatini, 2012; Wullschleger et al., 2006). On the other hand, the Hippo pathway exerts opposite effects, inhibiting cellular growth and proliferation and inducing cell death (Pan, 2010; Yu and Guan, 2013). This implies that tight coordination of these two pathways is important for the regulation of organ size and cellular integrity, and strongly suggests the existence of multiple cross-talk mechanisms between the mTOR and Hippo signaling cascades. However, mechanisms of regulation involving direct cross-talk between the Hippo and mTOR pathways remain unknown.

mTOR forms two functional multiprotein complexes, known as complex 1 (mTORC1) and complex 2 (mTORC2), by interacting with specific adaptor proteins. Raptor and Rictor are the main components of mTORC1 and mTORC2, respectively, and their deletion causes selective disruption of their respective complexes (Laplante and Sabatini, 2012; Wullschleger et al., 2006). Most of what is known about the cellular functions and substrates of mTOR in mammals pertains to mTORC1. On the other hand, there is still little known about the biology of mTORC2. Homozygous systemic deletion of *rictor* is embryonically lethal (Guertin et al., 2006; Shiota et al., 2006; Yang et al., 2006) and inducible systemic Rictor disruption reduces life span (Lamming et al., 2014), suggesting that mTORC2 is involved in the regulation of important cellular mechanisms and functions in mammals. However, the cellular functions, substrates and molecular mechanisms regulated by mTORC2 in different tissues and organs still remain to be clarified.

The Hippo pathway is composed of a group of evolutionarily conserved protein kinases that inhibit cellular growth and promote apoptosis (Pan, 2010; Yu and Guan, 2013). The core component of this group of kinases is MST1, which phosphorylates and activates LATS kinases, which in turn phosphorylate and inhibit YAP1, a co-transcription factor that promotes proliferation and survival. The Hippo pathway is inhibited in several different

types of cancer cells, whereas it is activated during cellular stress, when it promotes cell cycle arrest and death (Pan, 2010; Yu and Guan, 2013). The mechanisms through which the Hippo pathway is regulated under both unstressed and stressed conditions are poorly understood.

Tight control over cellular growth and survival appears to be particularly important in the heart, where regulation of cardiac mass and cardiomyocyte survival is critical for homeostasis and adaptation to stress. The mTOR and Hippo pathways appear to be important regulators of cellular growth and survival in the heart as well. Previous studies demonstrated that mTORC1 promotes cardiac growth and preserves cardiac function in the adult heart through the inhibition of 4E-BP1 protein (Sciarretta et al., 2014; Shende et al., 2011; Tamai et al., 2013; Zhang et al., 2010; Zhu et al., 2013). In contrast, activation of MST1 promotes dilated cardiomyopathy, contributes to cardiomyocyte death during ischemic injury and inhibits cardiac growth (Del Re et al., 2014; Maejima et al., 2013; Yamamoto et al., 2003). What is still unclear is the importance of mTORC2 in the regulation of cellular growth and survival in the heart, as well as how MST1 activity is controlled in the heart.

In the present study, we show that mTORC2 is a negative regulator of MST1 activity in the heart. We found that mTORC2 preserves cardiac structure and function and compensatory growth in response to mechanical stress by restraining the activity of MST1. Three main aspects of this study establish its relevance. The role of mTORC2 in the regulation of cardiomyocyte survival and size in the heart was elucidated. In addition, MST1 was identified as a substrate of mTORC2 in the regulation of cellular survival and growth. Finally, we discovered a mechanism of regulation of the Hippo pathway and a mechanism of direct cross-talk between the mTOR and Hippo pathways.

Results

mTORC2 is required for the maintenance of cardiac dimensions and function and for the left ventricular growth in response to pressure overload

We dissected the role of mTORC2 in the heart using a Cre/LoxP strategy to conditionally delete the *rictor* gene in cardiomyocytes (Shiota et al., 2006). Flox mice carrying a *rictor* allele in which exon 3 is flanked by two LoxP sites were cross-bred with mice with cardiomyocyte-specific overexpression of Cre recombinase under the control of the α-myosin heavy chain (MHC) promoter. Mice with α-*MHC*-*Cre*-mediated homozygous deletion of *rictor* (R-cKO mice) displayed a significant reduction in the Rictor protein level in the heart with respect to control mice (Figure 1A). On the other hand, the Raptor protein level was unchanged in R-cKO mice (Figure 1A). R-cKO mice were born alive and developed normally. At 2 months of age, they did not display any difference in cardiac dimensions or function with respect to control mice (Figure S1). However, at 6 months of age, R-cKO mice exhibited significant cardiac dilation and a reduction of systolic function with respect to both control mice and mice with heterozygous *rictor* knockout (Figure 1B–C). R-cKO mice also showed a significant increase in cardiac fibrosis and apoptosis, as indicated by an increased percentage of TUNEL-positive cells (Figure 1D–F). These results indicate that mTORC2 is required for the maintenance of cardiac structure and function in

the adult heart. Of note, the fact that mice with heterozygous *rictor* knockout (*rictor* flox/+, α-*MHC-Cre*+) did not show significant cardiac abnormalities excludes the possibility that Cre overexpression alone was responsible for the cardiac phenotype of R-cKO mice.

Next, we subjected young R-cKO mice, which did not show baseline cardiac abnormalities, as described above, to transverse aortic constriction (TAC) , an intervention that imposes high blood pressure (pressure overload) on the left ventricle of the heart. After 4 weeks of pressure overload, both longitudinal and transverse sections of the hearts of R-cKO mice showed significant cardiac dilation and wall thinning (Figure 2A–B). Echocardiographic analyses also indicated that R-cKO mice show severe cardiac dilation, wall thinning and systolic dysfunction as compared to controls after TAC (Figure 2C–D, Figure S2A–C). R-cKO mice also showed more severe signs of heart failure after TAC, including a marked increase in lung weight and left ventricular end-diastolic pressure (Figure 2E; Figure S2D). TAC induced significant left ventricular hypertrophy in both R-cKO and control mice, as indicated by increases in left ventricular weight/tibia length. However, the TAC-induced left ventricular hypertrophy was attenuated in R-cKO mice as compared to controls (Figure 2F), suggesting a defect in the hypertrophic response to TAC in R-cKO mice. This result was also confirmed by assessment of the cardiomyocyte cross-sectional area, as evaluated using wheat germ agglutinin staining of left ventricular tissue sections, which showed that the increase in cell size after TAC is modestly but significantly attenuated in R-cKO mice with respect to controls (Figure 3A–B). Cardiac apoptosis was also significantly increased in the hearts of R-cKO mice after TAC, whereas fibrosis was similar in control mice (Figure 3C–F). Pressure overload induced increases in the percentage of Ki-67 positive cardiomyocytes in control mouse hearts. However, R-cKO mice displayed a lower percentage of Ki-67-positive cardiomyocytes, suggesting that cardiomyocyte proliferation in response to pressure overload is attenuated in R-cKO mice (Figure 3G–H). Overall, these results demonstrate that R-cKO mice develop severe heart failure in response to pressure overload. Although heart failure with cardiac dilation and dysfunction is commonly accompanied by left ventricular hypertrophy in order to reduce wall stress, such a compensatory hypertrophy was attenuated in R-cKO mice. This suggests that endogenous Rictor/mTORC2 plays a significant role in mediating cardiac hypertrophy in response to pressure overload.

Rictor/mTORC2 disruption promotes cardiac dysfunction and heart failure through deregulated activation of MST1

We then investigated the molecular mechanisms through which Rictor/mTORC2 regulates survival and growth of cardiomyocytes. To this end, we evaluated the potential downstream signaling pathways of mTORC2 in R-cKO and control mice at baseline and after 2 days of TAC, which represents an early phase of pressure overload. This early time point allows for evaluation of the signaling pathways initially modulated in response to TAC before heart failure develops and other pathways are secondarily altered. AKT phosphorylation at serine 473 was significantly increased after TAC with respect to baseline in control mice (Figure S3A, C), suggesting that mTORC2 is significantly and rapidly activated in response to pressure overload. As expected, we found that there was significantly less myocardial AKT phosphorylation at serine 473 in R-cKO mice at baseline and after TAC, whereas phosphorylation at threonine 308 was unchanged in R-cKO mice (Figure S3A, C–D).

mTORC1 activity, as evaluated by p70S6 kinase phosphorylation, was also increased after TAC but did not differ between R-cKO and control mice (Figure S3A, E). Phosphorylation of GSK-3β at serine 9 and FOXO1 at threonine 24, two main downstream targets of AKT, also did not differ between R-cKO mice and control mice during the early phase of TAC, although the protein level of GSK-3β was increased and FOXO1 phosphorylation was reduced in the hearts of R-cKO mice after 4 weeks of TAC (Figure S3A–B, F–I).

The myocardial activity of MST1, as evaluated by its autophosphorylation at threonine 183, was significantly increased in R-cKO mice as compared to control mice, both at baseline and after 2 days of TAC (Figure 4A, Figure S4A–B). MST1 phosphorylation remained higher in R-cKO mice even after 4 weeks of TAC (Figure 4B, Figure S4C). In addition, MST1 cleavage, a marker of strong MST1 and caspase activation, was markedly increased in the hearts of R-cKO mice after TAC (Figure 4B, Figure S4D). Phosphorylation of LATS2 and YAP, two major downstream components of the Hippo pathway, was also significantly increased in R-cKO mice with respect to control mice, both at baseline and in response to TAC (Figure S4E). MST1 is a main component of the Hippo pathway, which negatively regulates organ size through stimulation of apoptosis and inhibition of cell proliferation (Del Re et al., 2014; Maejima et al., 2013; Pan, 2010; Yamamoto et al., 2003; Yu and Guan, 2013). We previously demonstrated that cardiac-specific overexpression of MST1 in transgenic mice (Tg-MST1) promotes cardiac dilation and dysfunction associated with cardiac fibrosis, apoptosis and inhibition of compensatory cardiomyocyte growth (Yamamoto et al., 2003). The cardiac phenotype of Tg-MST1 was remarkably similar to that observed in R-cKO mice after TAC. We therefore hypothesized that R-cKO mice develop cardiac dysfunction and dilation through deregulated activation of MST1 kinase. In order to test this hypothesis, we cross-bred R-cKO mice with mice overexpressing dominant-negative MST1 (kinase-dead MST1) in a cardiomyocyte-specific manner (Yamamoto et al., 2003). MST1 inhibition by dominant-negative MST1 almost completely rescued the cardiac dysfunction observed in 6-month-old R-cKO mice at baseline (Figure 4C). In addition, we found that MST1 inhibition significantly rescued cardiac dysfunction and heart failure in young R-cKO mice after 4 weeks of TAC (Figure 4D–F). This result indicates that Rictor/mTORC2 disruption promotes cardiomyopathy and heart failure through MST1 activation.

Rictor/mTORC2 phosphorylates MST1 in the SARAH domain, thereby reducing its dimerization and activity

mTORC2 may regulate MST1 activity either directly or indirectly through the modulation of AKT activity. In fact, AKT was previously found to inhibit MST1 (Collak et al., 2012). Rictor knockdown in cardiomyocytes *in vitro* was associated with a marked activation of MST1 that could not be rescued by concomitant overexpression of constitutively active AKT (Figure S5). This result suggests that mTORC2 may regulate MST1 in cardiomyocytes independently of AKT. In addition, previous studies demonstrated that AKT1 knockout mice do not show any baseline cardiac abnormalities, whereas they develop a marked increase in cardiac hypertrophy with respect to control mice after TAC (DeBosch et al., 2006), which is different from the phenotype of R-cKO mice that show attenuated left ventricular hypertrophy after TAC. Therefore, we tested the hypothesis that mTORC2 can directly regulate MST1 activity. Rictor and MST1 were partially co-localized in

cardiomyocytes, mainly in the perinuclear region, which is consistent with the previously-reported localization of Rictor and MST1 in the endoplasmic reticulum (Boulbes et al., 2011; Maejima et al., 2013) (Figure 5A). In addition, we found that endogenous Rictor interacts with MST1 in the mouse heart *in vivo* and in cardiomyocytes *in vitro* (Figure 5B, Figure S6A).

Next, we evaluated whether mTORC2 can phosphorylate MST1. Since mTORC2 is a multiprotein complex composed of several proteins that are required for its activity, in order to test whether mTORC2 can phosphorylate specific substrates we needed to purify mTORC2 from a biological system by immunoprecipitating Rictor, incubate it with a specific substrate and perform *in vitro* kinase assays (Sarbassov et al., 2005). We used kinase-dead MST1 as a substrate to avoid the strong MST1 autophosphorylation that is usually observed when wild-type MST1 is used in kinase assays (Maejima et al., 2013). Phosphorylation of MST1 by mTORC2 was unaffected by an AKT inhibitor but was abrogated by Torin1, an mTOR-specific inhibitor (Thoreen et al., 2009) (Figure 5C). These results suggest that mTORC2 phosphorylates MST1 through an mTOR-dependent but AKT-independent mechanism. In order to identify the MST1 phosphorylation site, mass spectrometry analysis was conducted on recombinant MST1 phosphorylated by mTORC2. The result of the mass spectrometry analysis indicated that mTORC2 phosphorylates MST1 at serine 438 (Figure 5D). This residue of MST1 is evolutionarily conserved across different species, although serine may be substituted with threonine in non-mammalian species (Figure 5E). Serine 438 is located in the SARAH domain of MST1 (Figure 5F), which is highly conserved from lower organisms to mammals and is of crucial importance for MST1 dimerization, autophosphorylation and subsequent activation (Praskova et al., 2004).

Using an antibody that is specific against MST1 phosphorylated at serine 438 (Figure S6B–D), we confirmed that mTORC2 phosphorylates MST1 at serine 438, after mTORC2 kinase reaction using recombinant MST1 as a substrate (Figure 5G). We also found that phosphorylation of MST1 at this site is significantly reduced in the hearts of R-cKO mice (Figure 5H; Figure S4F) and in cardiomyocytes with Rictor depletion *in vitro* (Figure S5). On the other hand, phosphorylation of MST1 at serine 438 was significantly increased in response to TAC, suggesting that MST1 phosphorylation by mTORC2 is increased during cardiac stress (Figure 5H; Figure S4F). Interestingly, we found that insulin, a known activator of mTORC2 (Lamming et al., 2012; Xie et al., 2011) and cellular growth, induces MST1 phosphorylation at serine 438 in cardiac fibroblasts. In contrast, mTOR inhibition by Torin1 significantly inhibited serine 438 phosphorylation and induced a marked increase in MST1 autophosphorylation (Figure S6E). These results suggest that mTORC2 also regulates and phosphorylates MST1 in other cell types as well as in cardiomyocytes and that serine 438 phosphorylation negatively regulates MST1 activation.

Since MST1 was dramatically activated and autophosphorylated in R-cKO mice, we hypothesized that MST1 phosphorylation at serine 438 by endogenous mTORC2 may interfere with the dimerization and activation of MST1. To test this hypothesis, wild-type, serine 438 phosphorylation-resistant mutant and serine 438 phosphorylation-mimicking mutant MST1, with either MYC or FLAG tags, were expressed in cells in different combinations, and co-immunoprecipitation assays were conducted. The dimeric interaction

between phosphomimetic MST1 mutant (S438D) and wild-type MST1 was significantly less than that between two wild-type MST1 proteins or between phosphoresistant MST1 mutant (S438A) and wild-type MST1 (Figure 6A). These results indicate that phosphorylation of MST1 at serine 438 interferes with MST1 dimerization.

Overexpression of either wild-type or S438A MST1 was able to significantly increase the phosphorylation of the downstream target LATS2 in cardiomyocytes. In contrast, S438D MST1 failed to induce significant phosphorylation of LATS2 (Figure 6B–C). Finally, overexpression of either wild-type or S438A MST1 significantly reduced cardiomyocyte survival. On the other hand, overexpression of S438D MST1 in cardiomyocytes failed to induce significant cell death (Figure 6D). Overall, these results indicate that mTORC2-dependent phosphorylation of MST1 at serine 438 inhibits MST1 homodimerization and activity, as well as MST1-induced cell death.

Discussion

The mTOR kinase is a master regulator of cellular growth and survival (Laplante and Sabatini, 2012; Wullschleger et al., 2006). However, the cellular processes and downstream signaling pathways specifically regulated by mTORC2 still remain to be clarified. Here we demonstrate the existence of a direct connection between mTORC2 and the Hippo pathway. Disruption of mTORC2 leads to deregulated activation of MST1 that causes cardiomyocyte apoptosis and cardiac dysfunction while, at the same time, suppressing compensatory myocardial growth. Thus, our study provides evidence indicating that mTORC2 promotes cellular growth and survival by restraining MST1 activity. In addition, we clarified a direct signaling link between the mTOR and Hippo pathways that is crucial for the preservation of cardiac function and growth in response to stress.

mTORC2 phosphorylates MST1 at serine 438 in the SARAH domain and reduces its ability to homodimerize and become activated. The SARAH domain is a highly conserved module located in the C-terminal portion of MST1 that is necessary for homodimerization (Praskova et al., 2004). The SARAH domain is also involved in heterodimerization with other SARAH domain-containing scaffolds, including RASSF1A, NORE1 and SAV1 that regulate MST1 activity as well (Pan, 2010; Praskova et al., 2004; Yu and Guan, 2013). A previous crystallographic analysis of the MST1 SARAH domain homo-dimer indicated that serine 438 is located between helix h1 and helix h2 and, together with tryptophan 439, it forms a bifurcated hydrogen bond with phenylalanine 435 (Hwang et al., 2007). This bifurcated hydrogen bond formation plays an important role in stabilizing the kinked conformation of helix h1 against helix h2, which in turn facilitates the autophosphorylation of the kinase domain of MST1. We speculate that phosphorylation of serine 438 may disturb the kinked conformation of the helix h1/h2, thereby interfering with both the MST1 homo-dimerization and autophosphorylation. In addition, the crystallographic structure of the homo-dimer of MST1 SARAH domains (Hwang et al., 2007) also suggests that serine 438 on one molecule of MST1 is located close to the aspartate 475 and glutamate 478 residues located on the other molecule of MST1. Thus, phosphorylation of serine 438 would interfere with the dimerization of MST1 through electrostatic repulsion (Figure S6F). Finally, as already

mentioned, it is also possible that phosphorylation of serine 438 would modulate the ability of MST1 to hetero-dimerize with RASSF/SAV1 proteins.

Previous studies indicated that, at physiological levels, Hippo signaling controls cellular growth and maintains organ structure, whereas deregulated Hippo signaling activation during stress is maladaptive and causes apoptosis and cell death (Pan, 2010; Yu and Guan, 2013). We believe that an important function of mTORC2 is to be a “guardian” of MST1 activity, finely controlling when MST1 activation is physiological or detrimental. In this regard, we observed that MST1 activity is increased in the hearts of wild-type mice during pressure overload. MST1 is activated under this condition through several upstream molecules, such as RASSF1a and K-RAS, which were previously found to mediate MST1 activation during cardiac stress (Del Re et al., 2010; Del Re et al., 2014). However, we found that mTORC2-dependent phosphorylation of MST1 is also increased during pressure overload, and that when mTORC2 is disrupted, MST1 activity further increases and cardiac dysfunction occurs. This suggests that the activity of mTORC2 toward MST1 is increased under this condition in order to maintain MST1 activation within physiological limits and preserve cardiac function. Other molecules also appear to have similar functions, acting to keep the level of activity of MST1 low. For example, NORE1 was shown to restrain MST1 activity *in vivo* (Praskova et al., 2004). In addition, previous work indicated that Raf-1 protein inhibits apoptosis and promotes cell survival by preventing the dimerization and activation of MST2 (O'Neill et al., 2004). Our study significantly extends this evidence and demonstrates that phosphorylation of MST1 by mTORC2 is another mechanism for limiting MST1 activity. Of note, this inhibitory mechanism appears to be specific for MST1, since the other MST isoform, MST2, lacks the serine 438 site in its primary structure. In addition, recent evidence indicates that MST2 exerts pro-hypertrophic effects in cardiomyocytes and does not regulate cardiac function in response to pressure overload (Zi et al., 2014). This diverges from the known anti-hypertrophic and pro-heart failure effects of MST1 in the heart and from the cardiac effects of mTORC2 disruption, as we demonstrated in our study. This prior evidence coupled with our results suggest that the detrimental effects of mTORC2 disruption are mediated by MST1 activation whereas MST2 is likely not involved but warrants further study.

mTORC2 positively regulates cellular growth and survival, mainly through the positive regulation of AKT (Jacinto et al., 2006; Jacinto et al., 2004; Sarbassov et al., 2005). The mTORC2/AKT pathway was also found to be associated with cardiomyocyte protection during ischemic injury (Volkers et al., 2013; Yano et al., 2014). We believe that our study significantly expands upon this evidence by demonstrating that mTORC2 is also able to regulate cellular growth and survival in specific cell types and conditions through the direct inhibition of MST1. Of note, previous evidence from Guan’s laboratory indicated that YAP, a main target of inhibition by the Hippo pathway, can activate AKT through miR-29-mediated inhibition of PTEN (Tumaneng et al., 2012). This data, combined with our results, indicates that mTORC2 can regulate AKT activity both directly and indirectly through the inhibition of the Hippo pathway and the resulting activation of YAP. In addition, AKT and MST1 were previously shown to mutually inhibit each other (Cinar et al., 2011; Collak et al., 2012). Thus, the mTORC2 and Hippo pathways can engage in crosstalk at multiple

levels. Of note, mTORC2 was also shown to activate SGK1 and PKC-α (Facchinetti et al., 2008; Garcia-Martinez and Alessi, 2008; Ikenoue et al., 2008). However, it is very unlikely that these factors are involved in the detrimental effects of mTORC2 deletion in the heart, since inhibition of either SGK1 or PKC-α protects the heart against hemodynamic stress (Braz et al., 2004; Das et al., 2012).

We believe that the molecular mechanisms presented in our study have broad biological implications. mTORC2 was previously shown to positively regulate survival of cancer cells (Laplante and Sabatini, 2012). On the other hand, the components of the Hippo pathway are onco-suppressors that are inhibited in different types of cancer (Pan, 2010). Our study suggests that mTORC2 may regulate carcinogenesis through the inhibition of Hippo signaling. In this regard, recent work reporting the results of a large-scale proteomics analysis of the human kinome conducted in leukemia, colon and breast cancer cell lines showed that MST1 is phosphorylated at serine 438 in all these cancer cell lines, whereas MST1 autophosphorylation could not be detected, indicating MST1 inhibition (Oppermann et al., 2009). These results are consistent with our evidence indicating that phospho-serine 438 inhibits MST1 activity. Notably, mTORC2 was shown to mediate survival of leukemia, colon and breast cancer cell lines (Laplante and Sabatini, 2012; Wullschleger et al., 2006).

Another potential and relevant implication of the connection between mTORC2 and the Hippo pathway relates to the control of cytoskeleton organization. mTORC2 was previously shown to promote actin polymerization and F-actin accumulation, through which it regulates cell migration and proliferation (Jacinto et al., 2004). On the other hand, the components of the Hippo pathway exhibit opposite effects on cytoskeleton organization, inhibiting actin polymerization and F-actin accumulation (Fernandez et al., 2011). Our results suggest that mTORC2 may also promote actin formation indirectly through inhibition of the Hippo pathway. F-actin accumulation induced by mTORC2 may also represent an indirect mechanism of regulation of the Hippo pathway by mTORC2, since actin polymerization results in Hippo signaling inhibition and YAP1 activation (Aragona et al., 2013; Zhao et al., 2012).

Our data may also be relevant to completely different biological systems and organisms. For example, amphibians are among the organisms with the highest regenerative capacity. The frog *Xenopus Laevi* was shown to be able to regenerate amputated limbs through the activation of YAP, suggesting Hippo pathway inhibition (Hayashi et al., 2014). Of note, in the MST1 homolog in *X. Laevi*, serine 438 is substituted with aspartic acid, suggesting a lower MST1 activity, which is consistent with an increased regenerative ability.

In conclusion, our study demonstrates the existence of crosstalk between the mTORC2 and Hippo pathways. We believe that the mTORC2/MST1 signaling cascade is a critical regulator of cell survival and growth in cardiomyocytes and, potentially, in other biological systems (Figure 6E).

Experimental procedures

Animal models

The generation of Rictor flox mice was previously described (Shiota et al., 2006). Rictor exon 3 was targeted in these animals. Flox mice were cross-bred with α-MHC-Cre transgenic mice in order to generate R-cKO mice. α-MHC-DN-MST1 (K59R) transgenic mice (C57BL/6J background) were previously described (Yamamoto et al., 2003). R-cKO mice were cross-bred with Tg-DN-MST1 mice. All mice were studied on a C57BL/6J background. Control (CT), R-cKO and R-cKO+DN-MST1 mice were subjected to TAC to induce pressure overload, as previously described (Yamamoto et al., 2003). Briefly, mice were anesthetized with pentobarbital sodium. The left chest was opened and mice were ventilated. Aortic constriction was performed by ligation of the transverse thoracic aorta with a 26-gauge needle using a 7-0 braided polyester suture. Echocardiographic and hemodynamic analyses were performed as previously described (Maejima et al., 2013; Yamamoto et al., 2003). All protocols concerning animal use were approved by the Institutional Animal Care and Use Committee at Rutgers-New Jersey Medical School.

Cell cultures, plasmid constructs, transfection and adenovirus generation

Primary cultures of ventricular cardiomyocytes were prepared from 1-day-old Crl: (WI) BR Wistar rats (Charles River Laboratories) as described (Maejima et al., 2013). Percoll gradient centrifugation was performed to separate the cardiomyocyte fraction from other cellular fractions. Cells were cultured in Dulbecco's modified Eagle's medium (DMEM)/ F-12 medium. HEK293 cells and COS7 cells were maintained as previously described (Maejima et al., 2013). Neonatal rat cardiac fibroblasts were isolated, passaged and maintained as previously described (Del Re et al., 2010). MYC-Rictor expression construct was from Addgene (Sarbassov et al., 2004). WT-MST1, AKT1, S438A-MST1 and S438D-MST1 cDNAs were subcloned into pDC316 vector (Maejima et al., 2013; Morisco et al., 2001; Yamamoto et al., 2003). Lipofectamine 2000 (Invitrogen) was used for transfection. Adenovirus vector generation was conducted as described (Yamamoto et al., 2003). The ΔE1 adenoviral genome incorporated in pBHGloxΔE1,3Cre (Microbix) was co-transfected with the pDC316 shuttle vector harboring the cDNA of interest into HEK293 cells.

Immunoprecipitation and immunoblot analysis

Left ventricular tissue homogenates or cell cultures were lysed with CHAPS buffer (40 mM HEPES, pH 7.5, 120 mM NaCl, 1 mM EDTA, 0.3% CHAPS) for mTORC2 immunoprecipitation, or with IGEPAL CA-630 buffer (50 mM Tris-HCl, pH 7.4, 1% IGEPAL CA-630, 10 mM EDTA, 150 mM NaCl), together with a protease inhibitor cocktail (Sigma). For FLAG-DN-MST1 immunoprecipitation, cells were lysed with a buffer containing 50 mM Tris-HCl, pH 7.5, 300 mM NaCl, 1% Triton X-100, 0.5% deoxycholic acid, 1 mM EDTA and protease inhibitors.

Lysates were incubated with the specified antibody and the immunocomplexes were precipitated using A/G sepharose beads for at least 2 hours at 4 °C. After immunoprecipitation, the samples were washed five times and were used for *in vitro* kinase assay reactions or for immunoblotting after immunoprecipitate elution. Immunoblot analysis

was performed as previously described (Maejima et al., 2013). For this analysis, tissue or cellular samples were lysed in RIPA buffer with 0.1 mM Na_3VO_4, 1 mM NaF, 1 mM β-glycerophosphate and protease inhibitor cocktail from Sigma.

In vitro kinase assay

MYC-Rictor was immunoprecipitated from HEK293 cells to isolate mTORC2 as described (Dibble et al., 2009; Sarbassov et al., 2004; Treins et al., 2010). mTORC2 was incubated with purified FLAG-DN-MST1 in the presence of mTORC2 kinase buffer (25 mM HEPES, pH 7.4, 100 mM potassium acetate, 1 mM $MgCl_2$), together with 500 μM of ATP, with or without 10 μCi [γ-^{32}P] ATP per reaction for 20 minutes at 37 °C, as previously described (Dibble et al., 2009; Ikenoue et al., 2009; Sarbassov et al., 2006; Sarbassov et al., 2005). The AKT inhibitor 1L-6-Hydroxymethyl-chiro-inositol2-[(R)-2-O-methyl-3-O-octadecylcarbonate] (Biovision, Cat# 1701-1) or Torin1 (Tocris. Cat# 4247) was used when specified. Phosphorylated proteins were separated by SDS-PAGE and analyzed by autoradiography.

Mass spectrometry

After kinase reaction with recombinant MST1 protein (1 μg), the samples were separated by SDS-PAGE and the MST1 band was excised for in-gel trypsin digestion. The resulting peptides were subjected to LC-MS/MS analysis on the Orbitrap Velos tandem mass spectrometry instrument (Thermo Scientific) using a nano electrospray source with a spray voltage of 2KV. MS spectra were acquired in a positive ion mode. MS/MS spectra were acquired using collision-induced dissociation (CID) in a data-dependent manner. The lock mass was used for accurate mass measurements. The MS/MS spectra were searched against Swissprot human database using the Mascot search engine. The following search parameters were used: trypsin was selected as the enzyme with 1 missed cleavage; peptide precursor mass tolerance of 10 ppm; and MS/MS mass tolerance of 0.5 Da. Methionine oxidation, serine and threonine phosphorylation and cysteine carbamidomethylation were selected as variable modifications. The phosphopeptides and their phosphorylation sites were verified by the PhosphoRS software (Thermo Scientific).

Immunofluorescence and staining

Cellular and tissue immunofluorescence were conducted according to a previously described method (Maejima et al., 2013). Briefly, neonatal rat cardiomyocytes plated on chamber slides (Lab-Tek) were fixed with 4% paraformaldehyde and permeabilized with PBS containing 0.1% Triton X-100. Mouse left ventricles were fixed in formalin and sectioned at 10-μm thickness. Tissue sections were then subjected to deparaffinization and antigen unmasking using citrate buffer and washed with PBS containing 0.3% Triton X-100. Samples were then blocked for 1 hour with PBS containing 5% bovine serum albumin *in vitro* experiments or with normal goat serum *in vivo*, and then incubated with primary antibody overnight. Cells were then incubated with Alexa 488- and Alexa 568-conjugated secondary antibodies (Invitrogen) for 3 hours. Nuclei were stained with DAPI. Images were taken using either conventional or confocal microscopy. For TUNEL staining, we used the In Situ Cell Death Detection kit (Roche) according to the manufacturer's instructions.

Masson's trichrome, hematoxylin and eosin and wheat germ agglutinin staining were conducted as previously described (Del Re et al., 2013; Maejima et al., 2013).

Cell survival assay

Cardiomyocyte survival was assessed using the CellTiter-Blue assay from Promega, according to the manufacturer's instructions.

Antibodies

Polyclonal antibody against MST1 phosphorylated at serine 438 was raised in rabbits and generated by 21st Century Biochemicals, Inc. The immunizing peptides were GDYEFLK[pS]WTVEDL and DYEFLK[pS]WTVEDLQ. Phospho-LATS2 (Thr1041) was kindly provided by Dr. Nojima, Osaka University. Other commercially available antibodies used in the study include: Rictor, MST1 (P-Thr183), MST1 (N-terminal), Raptor, AKT1 (P-Ser473), AKT1 (P-Thr308), AKT1, p70S6K (P-Thr389), GSK-3β (P-Ser9), GSK-3β, FOXO1 (P-Thr32/24), FOXO1, YAP1 (Ser127), YAP1, GAPDH, anti-mouse, anti-rabbit, conformation-specific anti-rabbit and FLAG from Cell Signaling; MST1 (C-terminal) from BD transduction; p70S6K and Rictor from Santa Cruz; FLAG, FLAG-agarose beads, MYC and Tubulin from Sigma; Rictor and LATS2 from Bethyl Laboratories; Ki-67 from Vector Laboratories; Troponin T from Neomarkers; and Alexa Fluor-488 Donkey Anti-Goat IgG, Alexa Fluor 488 Goat Anti-Rabbit IgG, Alexa Fluor-594 Goat Anti-Mouse IgG and Alexa Fluor-568 Donkey Anti-Mouse IgG from Invitrogen.

Statistics

Data are expressed as mean ± SEM. The t-test was used when the difference in means between 2 groups was evaluated. One-way ANOVA followed by the Bonferroni post hoc test was used when the comparison analysis was extended to multiple groups. Statistical analyses were performed with the use of GraphPad-Prism 5.00 (GraphPad-Software, San Diego, CA). P values of <0.05 were considered statistically significant.

Supplementary Material

Refer to Web version on PubMed Central for supplementary material.

Acknowledgements

The authors wish to thank Daniela Zablocki and Christopher D. Brady for critical reading of the manuscript.

Sources of funding

This work was supported in part by U.S. Public Health Service Grants HL102738, HL67724, HL91469, AG23039 and HL112330. This work was also supported by the Foundation Leducq Transatlantic Networks of Excellence. SS received support from a Postdoctoral Fellowship from the Founders Affiliate, American Heart Association and a grant from the Italian Society of Hypertension and from the Italian Society of Cardiology.

References

Aragona M, Panciera T, Manfrin A, Giulitti S, Michielin F, Elvassore N, Dupont S, Piccolo S. A mechanical checkpoint controls multicellular growth through YAP/TAZ regulation by actin-processing factors. Cell. 2013; 154:1047–1059. [PubMed: 23954413]

Boulbes DR, Shaiken T, Sarbassov dos D. Endoplasmic reticulum is a main localization site of mTORC2. Biochem Biophys Res Commun. 2011; 413:46–52. [PubMed: 21867682]

Braz JC, Gregory K, Pathak A, Zhao W, Sahin B, Klevitsky R, Kimball TF, Lorenz JN, Nairn AC, Liggett SB, et al. PKC-alpha regulates cardiac contractility and propensity toward heart failure. Nat Med. 2004; 10:248–254. [PubMed: 14966518]

Cinar B, Collak FK, Lopez D, Akgul S, Mukhopadhyay NK, Kilicarslan M, Gioeli DG, Freeman MR. MST1 is a multifunctional caspase-independent inhibitor of androgenic signaling. Cancer Res. 2011; 71:4303–4313. [PubMed: 21512132]

Collak FK, Yagiz K, Luthringer DJ, Erkaya B, Cinar B. Threonine-120 phosphorylation regulated by phosphoinositide-3-kinase/Akt and mammalian target of rapamycin pathway signaling limits the antitumor activity of mammalian sterile 20-like kinase 1. J Biol Chem. 2012; 287:23698–23709. [PubMed: 22619175]

Das S, Aiba T, Rosenberg M, Hessler K, Xiao C, Quintero PA, Ottaviano FG, Knight AC, Graham EL, Bostrom P, et al. Pathological role of serum- and glucocorticoid-regulated kinase 1 in adverse ventricular remodeling. Circulation. 2012; 126:2208–2219. [PubMed: 23019294]

DeBosch B, Treskov I, Lupu TS, Weinheimer C, Kovacs A, Courtois M, Muslin AJ. Akt1 is required for physiological cardiac growth. Circulation. 2006; 113:2097–2104. [PubMed: 16636172]

Del Re DP, Matsuda T, Zhai P, Gao S, Clark GJ, Van Der Weyden L, Sadoshima J. Proapoptotic Rassf1A/Mst1 signaling in cardiac fibroblasts is protective against pressure overload in mice. J Clin Invest. 2010; 120:3555–3567. [PubMed: 20890045]

Del Re DP, Matsuda T, Zhai P, Maejima Y, Jain MR, Liu T, Li H, Hsu CP, Sadoshima J. Mst1 promotes cardiac myocyte apoptosis through phosphorylation and inhibition of Bcl-xL. Mol Cell. 2014; 54:639–650. [PubMed: 24813943]

Del Re DP, Yang Y, Nakano N, Cho J, Zhai P, Yamamoto T, Zhang N, Yabuta N, Nojima H, Pan D, et al. Yes-associated protein isoform 1 (Yap1) promotes cardiomyocyte survival and growth to protect against myocardial ischemic injury. J Biol Chem. 2013; 288:3977–3988. [PubMed: 23275380]

Dibble CC, Asara JM, Manning BD. Characterization of Rictor phosphorylation sites reveals direct regulation of mTOR complex 2 by S6K1. Mol Cell Biol. 2009; 29:5657–5670. [PubMed: 19720745]

Facchinetti V, Ouyang W, Wei H, Soto N, Lazorchak A, Gould C, Lowry C, Newton AC, Mao Y, Miao RQ, et al. The mammalian target of rapamycin complex 2 controls folding and stability of Akt and protein kinase C. EMBO J. 2008; 27:1932–1943. [PubMed: 18566586]

Fernandez BG, Gaspar P, Bras-Pereira C, Jezowska B, Rebelo SR, Janody F. Actin-Capping Protein and the Hippo pathway regulate F-actin and tissue growth in Drosophila. Development. 2011; 138:2337–2346. [PubMed: 21525075]

Garcia-Martinez JM, Alessi DR. mTOR complex 2 (mTORC2) controls hydrophobic motif phosphorylation and activation of serum- and glucocorticoid-induced protein kinase 1 (SGK1). Biochem J. 2008; 416:375–385. [PubMed: 18925875]

Guertin DA, Stevens DM, Thoreen CC, Burds AA, Kalaany NY, Moffat J, Brown M, Fitzgerald KJ, Sabatini DM. Ablation in mice of the mTORC components raptor, rictor, or mLST8 reveals that mTORC2 is required for signaling to Akt-FOXO and PKCalpha, but not S6K1. Dev Cell. 2006; 11:859–871. [PubMed: 17141160]

Hayashi S, Tamura K, Yokoyama H. Yap1, transcription regulator in the Hippo signaling pathway, is required for Xenopus limb bud regeneration. Dev Biol. 2014; 388:57–67. [PubMed: 24491818]

Hwang E, Ryu KS, Paakkonen K, Guntert P, Cheong HK, Lim DS, Lee JO, Jeon YH, Cheong C. Structural insight into dimeric interaction of the SARAH domains from Mst1 and RASSF family proteins in the apoptosis pathway. Proc Natl Acad Sci U S A. 2007; 104:9236–9241. [PubMed: 17517604]

Ikenoue T, Hong S, Inoki K. Monitoring mammalian target of rapamycin (mTOR) activity. Methods Enzymol. 2009; 452:165–180. [PubMed: 19200882]

Ikenoue T, Inoki K, Yang Q, Zhou X, Guan KL. Essential function of TORC2 in PKC and Akt turn motif phosphorylation, maturation and signalling. EMBO J. 2008; 27:1919–1931. [PubMed: 18566587]

Jacinto E, Facchinetti V, Liu D, Soto N, Wei S, Jung SY, Huang Q, Qin J, Su B. SIN1/MIP1 maintains rictor-mTOR complex integrity and regulates Akt phosphorylation and substrate specificity. Cell. 2006; 127:125–137. [PubMed: 16962653]

Jacinto E, Loewith R, Schmidt A, Lin S, Ruegg MA, Hall A, Hall MN. Mammalian TOR complex 2 controls the actin cytoskeleton and is rapamycin insensitive. Nat Cell Biol. 2004; 6:1122–1128. [PubMed: 15467718]

Lamming DW, Mihaylova MM, Katajisto P, Baar EL, Yilmaz OH, Hutchins A, Gultekin Y, Gaither R, Sabatini DM. Depletion of Rictor, an essential protein component of mTORC2, decreases male lifespan. Aging Cell. 2014

Lamming DW, Ye L, Katajisto P, Goncalves MD, Saitoh M, Stevens DM, Davis JG, Salmon AB, Richardson A, Ahima RS, et al. Rapamycin-induced insulin resistance is mediated by mTORC2 loss and uncoupled from longevity. Science. 2012; 335:1638–1643. [PubMed: 22461615]

Laplante M, Sabatini DM. mTOR signaling in growth control and disease. Cell. 2012; 149:274–293. [PubMed: 22500797]

Maejima Y, Kyoi S, Zhai P, Liu T, Li H, Ivessa A, Sciarretta S, Del Re DP, Zablocki DK, Hsu CP, et al. Mst1 inhibits autophagy by promoting the interaction between Beclin1 and Bcl-2. Nat Med. 2013; 19:1478–1488. [PubMed: 24141421]

Morisco C, Seta K, Hardt SE, Lee Y, Vatner SF, Sadoshima J. Glycogen synthase kinase 3beta regulates GATA4 in cardiac myocytes. J Biol Chem. 2001; 276:28586–28597. [PubMed: 11382772]

O'Neill E, Rushworth L, Baccarini M, Kolch W. Role of the kinase MST2 in suppression of apoptosis by the proto-oncogene product Raf-1. Science. 2004; 306:2267–2270. [PubMed: 15618521]

Oppermann FS, Gnad F, Olsen JV, Hornberger R, Greff Z, Keri G, Mann M, Daub H. Large-scale proteomics analysis of the human kinome. Molecular & cellular proteomics : MCP. 2009; 8:1751–1764. [PubMed: 19369195]

Pan D. The hippo signaling pathway in development and cancer. Dev Cell. 2010; 19:491–505. [PubMed: 20951342]

Praskova M, Khoklatchev A, Ortiz-Vega S, Avruch J. Regulation of the MST1 kinase by autophosphorylation, by the growth inhibitory proteins, RASSF1 and NORE1, and by Ras. Biochem J. 2004; 381:453–462. [PubMed: 15109305]

Sarbassov DD, Ali SM, Kim DH, Guertin DA, Latek RR, Erdjument-Bromage H, Tempst P, Sabatini DM. Rictor, a novel binding partner of mTOR, defines a rapamycin-insensitive and raptor-independent pathway that regulates the cytoskeleton. Curr Biol. 2004; 14:1296–1302. [PubMed: 15268862]

Sarbassov DD, Ali SM, Sengupta S, Sheen JH, Hsu PP, Bagley AF, Markhard AL, Sabatini DM. Prolonged rapamycin treatment inhibits mTORC2 assembly and Akt/PKB. Mol Cell. 2006; 22:159–168. [PubMed: 16603397]

Sarbassov DD, Guertin DA, Ali SM, Sabatini DM. Phosphorylation and regulation of Akt/PKB by the rictor-mTOR complex. Science. 2005; 307:1098–1101. [PubMed: 15718470]

Sciarretta S, Volpe M, Sadoshima J. Mammalian target of rapamycin signaling in cardiac physiology and disease. Circ Res. 2014; 114:549–564. [PubMed: 24481845]

Shende P, Plaisance I, Morandi C, Pellieux C, Berthonneche C, Zorzato F, Krishnan J, Lerch R, Hall MN, Ruegg MA, et al. Cardiac raptor ablation impairs adaptive hypertrophy, alters metabolic gene expression, and causes heart failure in mice. Circulation. 2011; 123:1073–1082. [PubMed: 21357822]

Shiota C, Woo JT, Lindner J, Shelton KD, Magnuson MA. Multiallelic disruption of the rictor gene in mice reveals that mTOR complex 2 is essential for fetal growth and viability. Dev Cell. 2006; 11:583–589. [PubMed: 16962829]

Tamai T, Yamaguchi O, Hikoso S, Takeda T, Taneike M, Oka T, Oyabu J, Murakawa T, Nakayama H, Uno Y, et al. Rheb (Ras homologue enriched in brain)-dependent mammalian target of rapamycin complex 1 (mTORC1) activation becomes indispensable for cardiac hypertrophic growth after early postnatal period. J Biol Chem. 2013; 288:10176–10187. [PubMed: 23426372]

Thoreen CC, Kang SA, Chang JW, Liu Q, Zhang J, Gao Y, Reichling LJ, Sim T, Sabatini DM, Gray NS. An ATP-competitive mammalian target of rapamycin inhibitor reveals rapamycin-resistant functions of mTORC1. J Biol Chem. 2009; 284:8023–8032. [PubMed: 19150980]

Treins C, Warne PH, Magnuson MA, Pende M, Downward J. Rictor is a novel target of p70 S6 kinase-1. Oncogene. 2010; 29:1003–1016. [PubMed: 19935711]

Tumaneng K, Schlegelmilch K, Russell RC, Yimlamai D, Basnet H, Mahadevan N, Fitamant J, Bardeesy N, Camargo FD, Guan KL. YAP mediates crosstalk between the Hippo and PI(3)K-TOR pathways by suppressing PTEN via miR-29. Nat Cell Biol. 2012; 14:1322–1329. [PubMed: 23143395]

Volkers M, Konstandin MH, Doroudgar S, Toko H, Quijada P, Din S, Joyo A, Ornelas L, Samse K, Thuerauf DJ, et al. mTORC2 Protects the Heart from Ischemic Damage. Circulation. 2013

Wullschleger S, Loewith R, Hall MN. TOR signaling in growth and metabolism. Cell. 2006; 124:471–484. [PubMed: 16469695]

Xie X, Zhang D, Zhao B, Lu MK, You M, Condorelli G, Wang CY, Guan KL. IkappaB kinase epsilon and TANK-binding kinase 1 activate AKT by direct phosphorylation. Proc Natl Acad Sci U S A. 2011; 108:6474–6479. [PubMed: 21464307]

Yamamoto S, Yang G, Zablocki D, Liu J, Hong C, Kim SJ, Soler S, Odashima M, Thaisz J, Yehia G, et al. Activation of Mst1 causes dilated cardiomyopathy by stimulating apoptosis without compensatory ventricular myocyte hypertrophy. J Clin Invest. 2003; 111:1463–1474. [PubMed: 12750396]

Yang Q, Inoki K, Ikenoue T, Guan KL. Identification of Sin1 as an essential TORC2 component required for complex formation and kinase activity. Genes Dev. 2006; 20:2820–2832. [PubMed: 17043309]

Yano T, Ferlito M, Aponte A, Kuno A, Miura T, Murphy E, Steenbergen C. Pivotal role of mTORC2 and involvement of ribosomal protein S6 in cardioprotective signaling. Circ Res. 2014; 114:1268–1280. [PubMed: 24557881]

Yu FX, Guan KL. The Hippo pathway: regulators and regulations. Genes Dev. 2013; 27:355–371. [PubMed: 23431053]

Zhang D, Contu R, Latronico MV, Zhang JL, Rizzi R, Catalucci D, Miyamoto S, Huang K, Ceci M, Gu Y, et al. MTORC1 regulates cardiac function and myocyte survival through 4E–BP1 inhibition in mice. J Clin Invest. 2010; 120:2805–2816. [PubMed: 20644257]

Zhao B, Li L, Wang L, Wang CY, Yu J, Guan KL. Cell detachment activates the Hippo pathway via cytoskeleton reorganization to induce anoikis. Genes Dev. 2012; 26:54–68. [PubMed: 22215811]

Zhu Y, Pires KM, Whitehead KJ, Olsen CD, Wayment B, Zhang YC, Bugger H, Ilkun O, Litwin SE, Thomas G, et al. Mechanistic target of rapamycin (Mtor) is essential for murine embryonic heart development and growth. PLoS One. 2013; 8:e54221. [PubMed: 23342106]

Zi M, Maqsood A, Prehar S, Mohamed TM, Abou-Leisa R, Robertson A, Cartwright EJ, Ray SG, Oh S, Lim DS, et al. The mammalian Ste20-like kinase 2 (Mst2) modulates stress-induced cardiac hypertrophy. J Biol Chem. 2014; 289:24275–24288. [PubMed: 25035424]

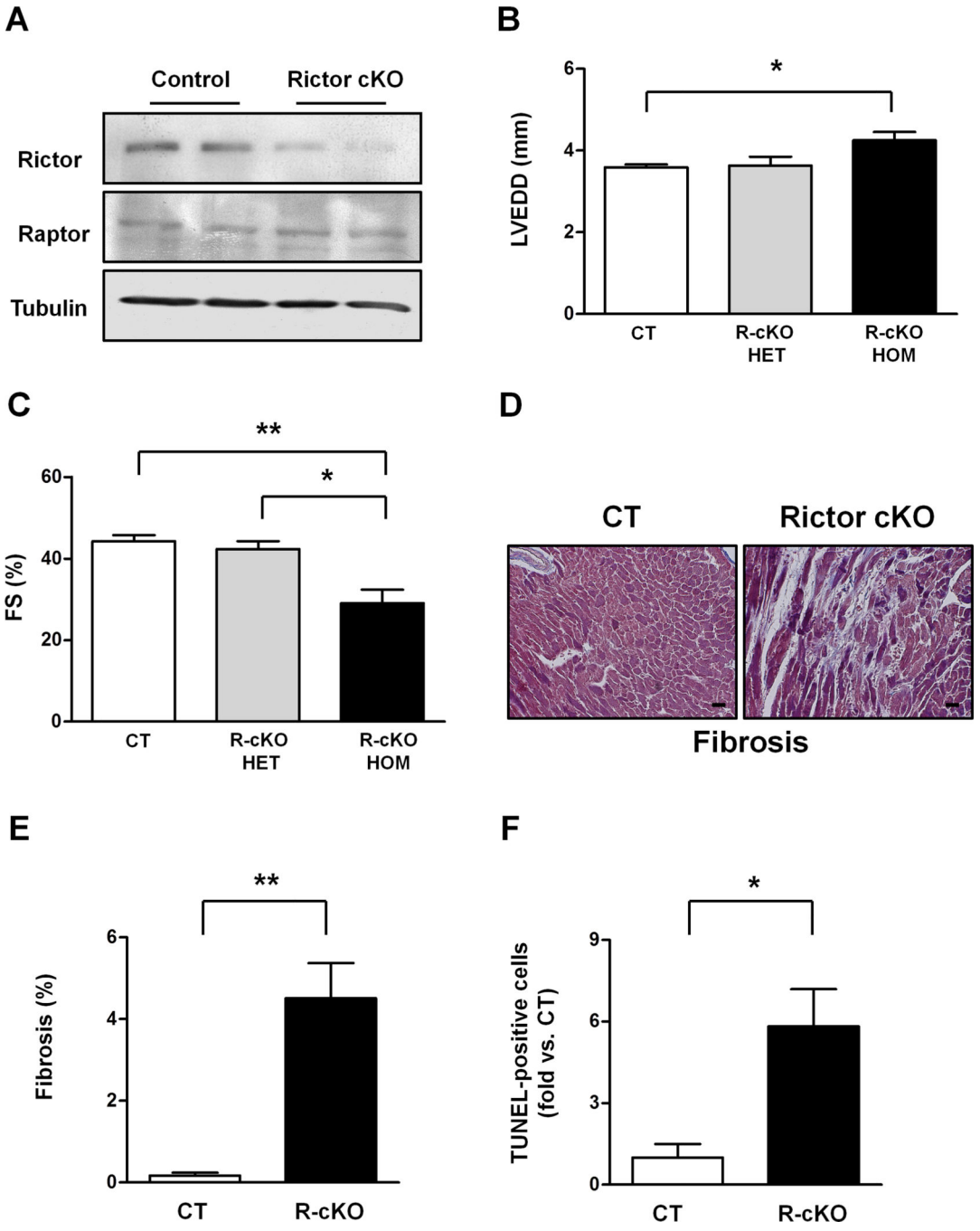

Figure 1. Rictor/mTORC2 disruption promotes progressive cardiac dysfunction and dilation

A. Representative immunoblot showing Rictor protein levels in control (CT) and Rictor knockout mice (R-cKO). **B–C**. Six-month-old CT and R-cKO mice (heterozygous and homozygous) underwent echocardiographic analysis. Left ventricular end-diastolic diameter (LVEDD) and fractional shortening (FS) were measured. N=3–8. **D–E**. Cardiac Masson's trichrome staining was performed in left ventricular sections from CT and R-cKO mice. Representative pictures (D) and fibrosis quantification (E) are shown. N=4. Scale bar= 50

μm. **F**. The percentage of TUNEL-positive cells was evaluated in the left ventricle of CT and R-cKO mice. N=3. All data are expressed as mean ± SEM * $p<0.05$; ** $p<0.01$.

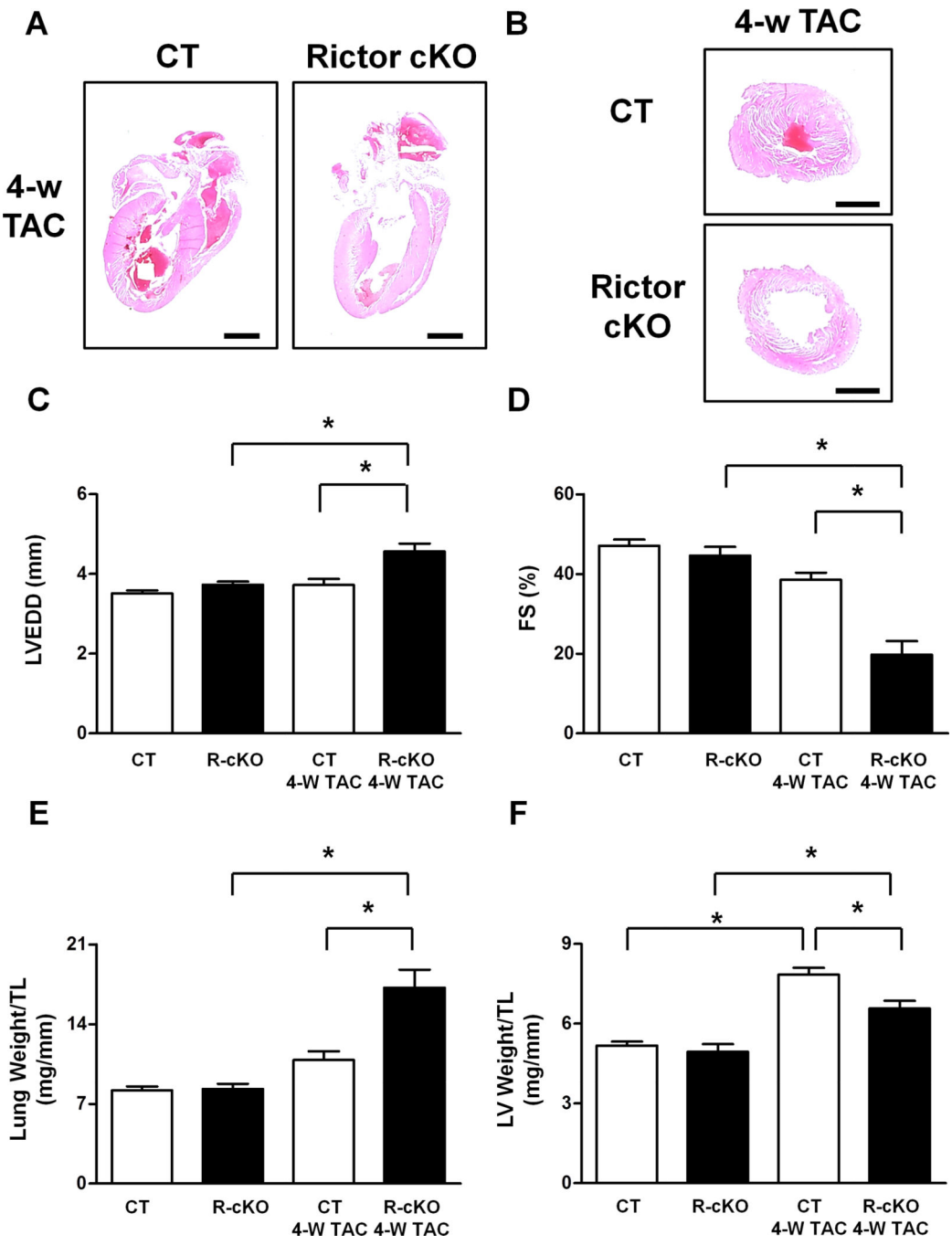

Figure 2. Rictor/mTORC2 disruption impairs cardiac adaptation to pressure overload

A–B. Hematoxylin and eosin staining was performed in longitudinal heart sections and transverse left ventricular sections from CT and R-cKO mice. Representative pictures are shown. Scale bar= 2 mm. **C–D**. CT and R-cKO mice underwent echocardiographic analysis. Left ventricular end-diastolic diameter (LVEDD) and fractional shortening (FS) were measured. N=7–8. **E–F**. Gravimetric analysis was conducted in CT and R-cKO mice. Lung (E) and left ventricular (F) weight normalized by tibial length were calculated. N=7–8. All data are expressed as mean ± SEM. * $p<0.05$; n.s.= not significant.

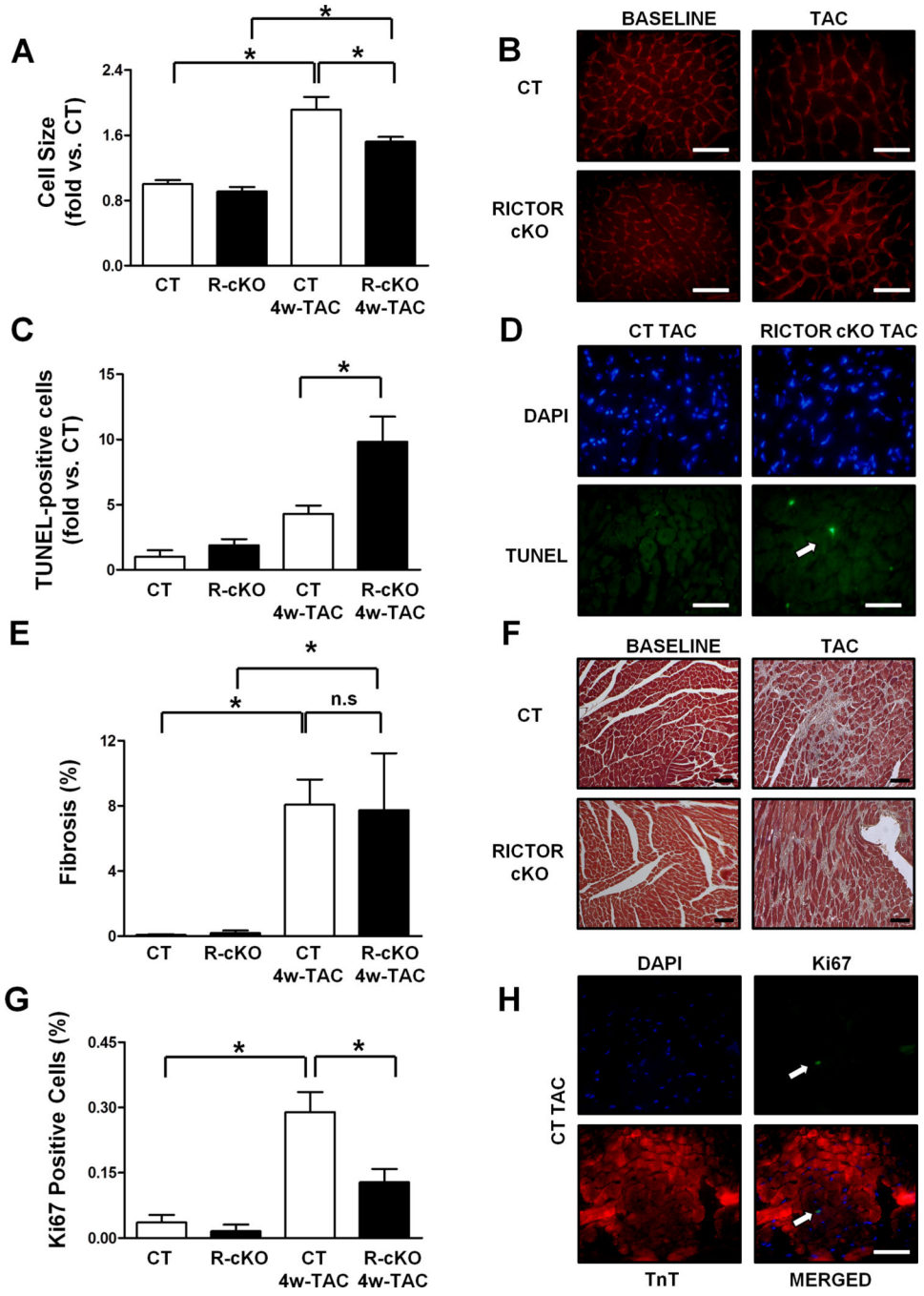

Figure 3. Rictor/mTORC2 disruption impairs left ventricular growth and promotes apoptosis in response to pressure overload

Wheat germ agglutinin, TUNEL, Masson's trichrome and Ki67 stainings were performed in left ventricular sections from CT and R-cKO mice at baseline and after 4 weeks of pressure overload. Representative pictures are shown (B, D, F, H). Cell size (A), percentage of TUNEL-positive cells (C), percentage of fibrosis (E) and percentage of Ki67-positive cells (G) were measured. N=3–5. All data are expressed as mean ± SEM and as fold vs. CT when specified. * $p<0.05$. Scale bar= 100 μm.

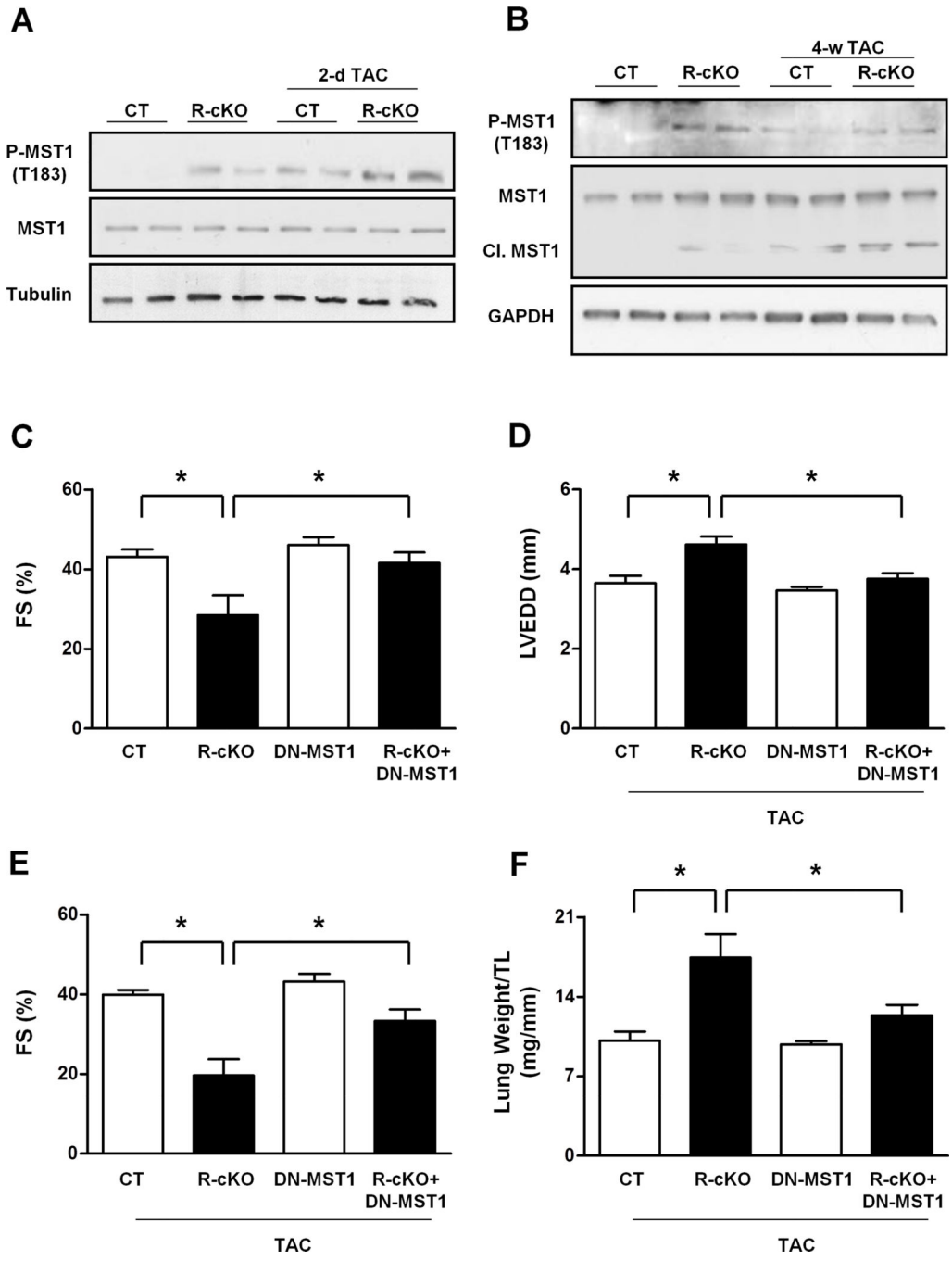

Figure 4. Rictor/mTORC2 disruption promotes cardiac dysfunction and dilation through MST1 activation

A–B. Phosphorylated, total and cleaved levels of MST1 were evaluated in the hearts of CT and R-cKO mice at baseline and after pressure overload. Representative immunoblots are shown, and densitometric analyses are shown in Figure S4. **C**. Six-month-old CT, R-cKO, DN-MST1 and R-cKO+DN-MST1 mice underwent echocardiographic analysis. Fractional shortening (FS) was measured. N=3–7. **D–F**. CT, R-cKO, DN-MST1 and R-cKO+DN-MST1 mice around 10 weeks of age were subjected to 4 weeks of TAC and then underwent

echocardiographic analysis. Left ventricular end-diastolic diameter (LVEDD) and fractional shortening (FS) were measured. N=3–7. All data are expressed as mean ± SEM * $p<0.05$.

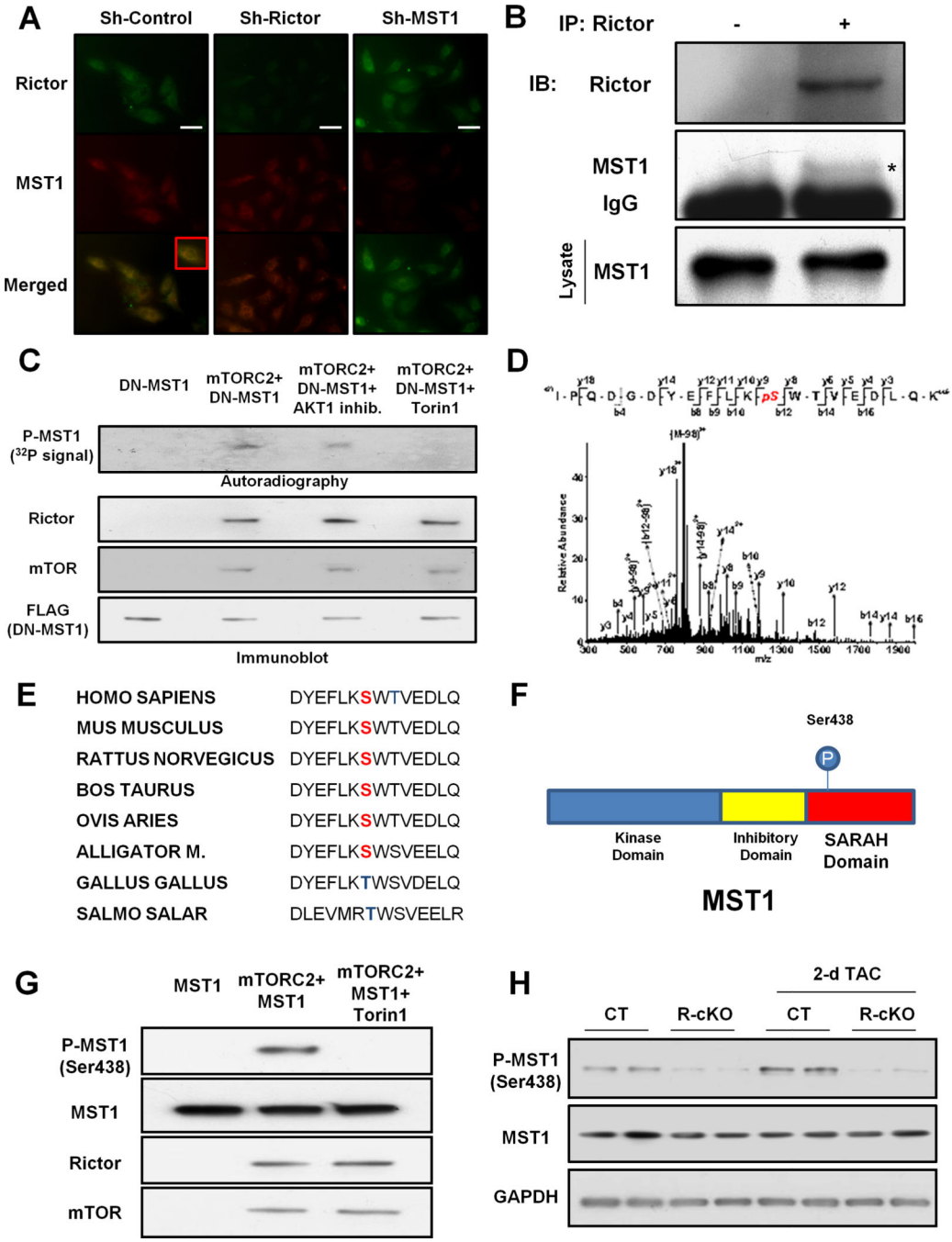

Figure 5. Rictor/mTORC2 phosphorylates MST1 at serine 438

A. Immunocytofluorescence assay of Rictor and MST1 was performed in neonatal rat cardiomyocytes transduced with either control adenovirus or an adenovirus expressing a short-hairpin sequence targeting Rictor or MST1. Representative pictures are shown. A higher magnification of a portion of the merged panel of control sample is shown in the inset. Scale bar: 50 μm. **B**. Rictor was immunoprecipitated from mouse left ventricle. Immunoprecipitate with control IgG was used as control. Representative immunoblots of Rictor and MST1 are shown. **C**. Kinase reaction was performed with the specified proteins.

Fifty μM of 1L-6-Hydroxymethyl-chiro-inositol2-[(R)-2-O-methyl-3-O-octadecylcarbonate] or 1 μM of Torin1 were used when specified. Representative autoradiograph is shown. A portion of the samples used in each kinase reaction was used for immunoblot analysis to test the levels of FLAG-DN-MST1, Rictor and mTOR. **D**. Analysis of the MST1 peptide by tandem mass spectrometry after incubation with the mTORC2 complex in a kinase reaction. **E**. Conservation of MST1 serine 438 across different species is shown. **F**. Schema representing the localization of the serine 438 residue in the MST1 SARAH domain. **G**. A kinase reaction was performed with recombinant MST1 in the presence or absence of mTORC2. Torin1 was used when specified. After the kinase reaction, MST1 phosphorylation at serine 438 was evaluated. **H**. Cardiac phosphorylation levels of MST1 at serine 438 were evaluated in CT and R-cKO at baseline and after TAC. Immunoblots are shown.

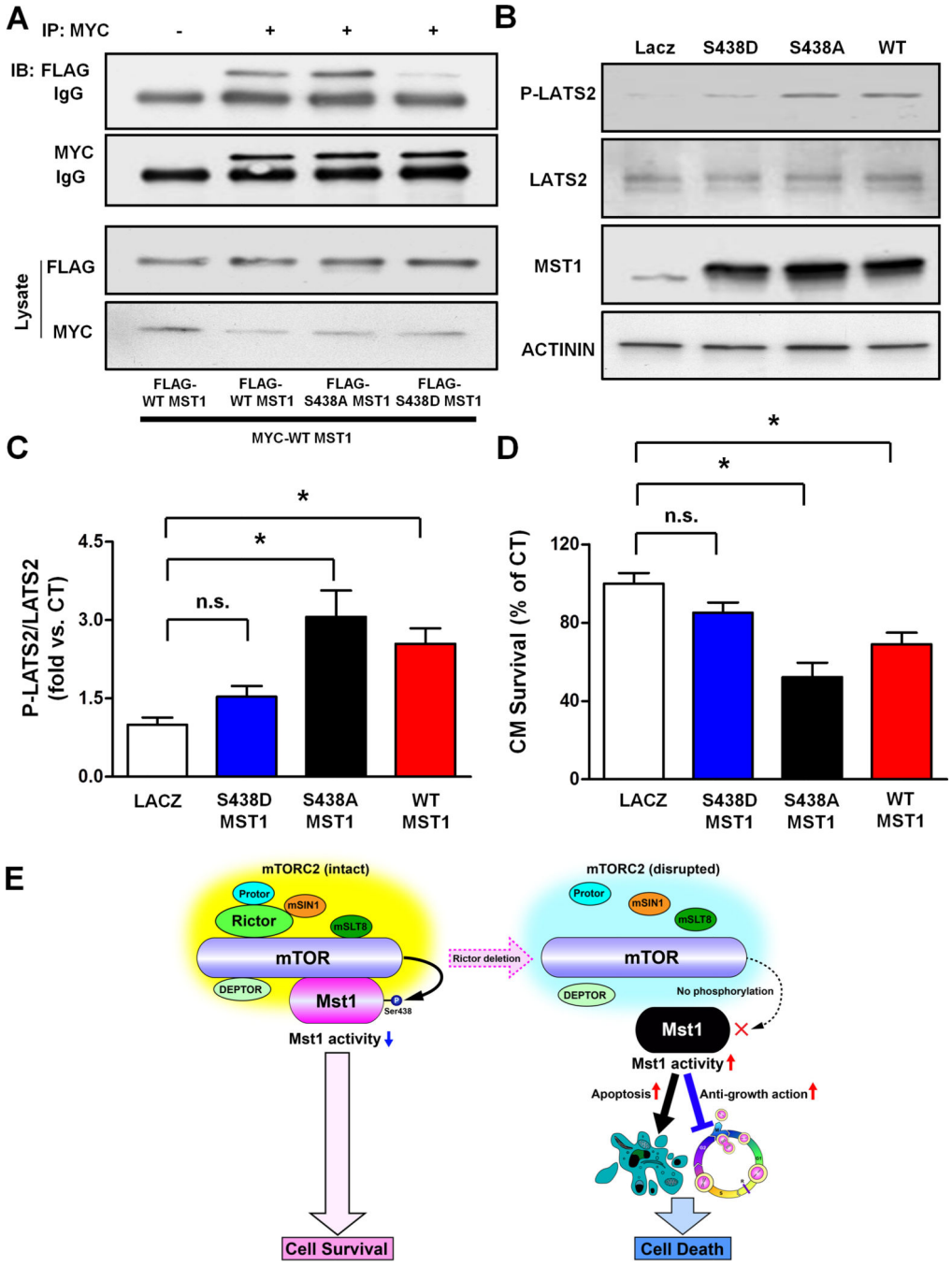

Figure 6. MST1 phosphorylation at serine 438 reduces its dimerization and activity

A. COS7 cells were transfected with the specified plasmids. MYC was immunoprecipitated and immunoblots for MYC and FLAG are shown. Immunoprecipitate with control IgG was used as a control. **B–C**. Cardiomyocytes were transduced with ad-LacZ, ad-FLAG-WT-MST1, ad-FLAG-S438A-MST1 or ad-FLAG-S438D-MST1. After 48 hours, the levels of phospho-LATS2 (T1041 homologous), total LATS2 and MST1 were evaluated and representative immunoblots are shown (B) together with quantification analysis of the P-LATS2/LATS2 ratio (C). N=3. **D**. After 72 hours, cardiomyocyte survival was assessed by

CellTiter-Blue assay. N=4. All the data are expressed as mean ± SEM * $p<0.05$; n.s.= not significant. **E**. Schema representing the negative regulation of MST1 by mTORC2, which preserves cell survival.